

CHANNEL CAPACITY ESTIMATION WITH RESPECT TO DISTANCE IN 5G MILLIMETER WAVE BANDS

Vaibhav Yavalkar^{1,2*}, Dr. Kamal Kumar Agarwal¹ and Dr. Sameer Nanivadekar²

^{1*} Pacific Academy of Higher Education and Research University, 313003,
Rajasthan, India.

^{2*} A. P. Shah Institute of Technology, 400615, Maharashtra.

Abstract

In the fast-evolving landscape of wireless communication, the demand for high-speed, reliable networks are escalating. Within this context, our research addresses a pivotal concern in 5G technology—channel capacity in millimeter-wave bands. Recognizing the challenges posed by distance-related path loss, we employed the MathWorks 5G NR CDL-A channel model to comprehensively analyze the interplay of carrier frequency, antenna heights, and link distances between Base Stations (BS) and User Equipment (UE). Our simulations, ranging from 6 GHz to 90 GHz, reveal a nuanced relationship between BS-UE horizontal distance and average channel capacity, crucial for optimizing network deployments. By exploring the implications of varying frequencies and presenting two scenarios—one with path loss effects only and another incorporating oxygen absorption—we contribute valuable insights for network engineers and policymakers. This work signifies a crucial step towards enhancing the efficiency and reliability of 5G millimeter-wave networks, fostering their societal impact by paving the way for more robust and responsive communication infrastructures.

Keywords: 5G, Bandwidth, Capacity estimation, NR, Channel

Introduction

Millimeter waves are high-frequency waves that are broadcast at frequencies between 30 and 300 gigahertz (GHz), compared to the bands below 6 GHz that were used for mobile devices in the past. They are called millimeter waves because they vary in length from 1 to 10 mm, compared to the radio waves that serve today smartphones, which measure tens of centimeters in length. The 5G spectrum utilizing millimeter-wave frequency bands starting at 24 GHz up to 100 GHz gives ultra-high speed, increased traffic, high capacity, with more connected devices in the cellular network. Millimeter waves have a limited propagation distance due to their high frequency and short wavelength.

As the distance between two communicators increases, the path loss value in mm Wave also increases. This means that as the distance between two communicators increases, the signal strength decreases, which can affect the quality of communication. Path loss refers to the reduction in power density (attenuation) of an electromagnetic wave as it propagates through space. As a result of path loss, the received signal power level is several orders below the transmitted power level. The

received power level is dependent on factors such as transmission power, antenna gains, frequency of operation and the distance between the transmitter and the receiver. Path loss is a major component in the analysis and design of the link budget of a telecommunication system.

Antenna gain is a measure of how well an antenna converts the input power into radio waves in a particular direction. In 5G millimeter-wave bands, antenna designs must take into consideration the high propagation loss due to atmospheric absorption at millimeter waves.

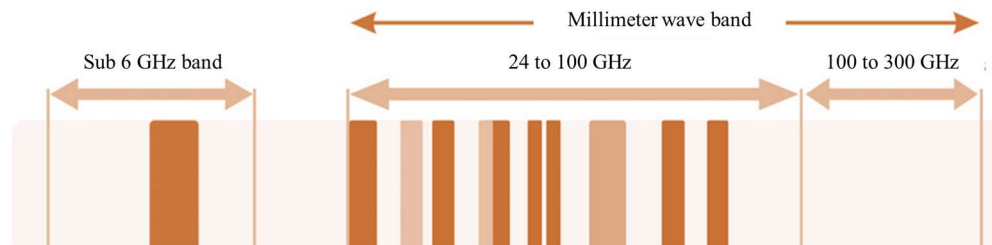


Fig. 1: 5G Communication band with Millimeter wave band

Literature Review

The 5G antennas are expected to have high gain, efficiencies and bandwidth greater than 1 GHz. For example, a microstrip patch antenna functioning at 28 GHz has been proposed with a measured gain of 7.4 dB [Wen et al \(2021\)](#).

The transmission power of a 5G base station can vary depending on several factors such as the frequency band used, the number of antennas, and the bandwidth. A 5G base station has a transmission power of 240 W for a bandwidth of 100 MHz and uses 64 transmission and 64 reception antennas [Han and Bian \(2020\)](#) .

Several noteworthy studies are discussed in the context of 5G millimeter wave bands and their channel capacity estimation concerning distance. [Abbas et al. \(2017\)](#) [Abbas et al \(2017\)](#) conducted a comparative analysis between their results and the 2.14 GHz LTE-A frequency band. The challenge of supporting multi-connectivity in mm-waves was highlighted, particularly the need for precise tracking of each link's direction, power, and timing. To tackle this challenge, [Giordani et al. \(2018\)](#) [Giordani et al \(2018\)](#) proposed a novel uplink measurement system. This system, aided by a local coordinator in the legacy band, enabled continuous monitoring of channel propagation conditions. Additionally, it facilitated the design of efficient control plane applications, including handover, beam tracking, and initial access. In addressing the issues with estimation efficiency and accuracy in the UM MIMO communication system, [Nie et al. \(2019\)](#) [Nie and Akyildiz \(2019\)](#) put forth a channel estimation method based on deep kernel learning. [Uwaechia](#)

et al. (2020) [Uwaechia and Mahyuddin \(2020\)](#) provided a comprehensive overview of emerging technologies for 5G systems, encompassing massive MIMO, multiple access technologies, hybrid analog- digital precoding and combining, non-orthogonal multiple access (NOMA), cell-free massive MIMO, and simultaneous wireless information and power transfer (SWIPT) technologies. Al-Samman et al. (2020) [Al-Samman et al \(2020\)](#) contributed to the field with ultra-wideband channel measurements for millimeter wave bands at 19, 28, and 38 GHz. Belgiovine et al. (2021) [Belgiovine et al \(2021\)](#) proposed the adoption of deep learning using a multi-layer perceptron architecture, surpassing the performance of traditional CSI processing methods like least square (LS) and linear minimum mean square error (LMMSE) estimation. This approach introduces a beyond fifth generation (B5G) networking paradigm where machine learning plays a pivotal role in driving networking optimization. Zheng et al. (2021) [Zheng et al \(2021\)](#) presented a field experiment on an E-band millimeter-wave link in Nanjing, China, contributing valuable insights to the research domain. In addition to the mentioned works, other influential studies include those conducted by Thomas et al. (2014) [Thomas and Vook \(2014\)](#) , Maruta et al. (2016) [Maruta et al \(2016\)](#) , and Wang et al. (2019) [Wang et al \(2019\)](#) . These works collectively contribute to the understanding of channel capacity estimation in 5G millimeter wave bands in relation to distance.

Experimental setup

This research aims to model Multiple Input Multiple Output (MIMO) channels by leveraging the Mathworks 5G NR CDL channel model within the 5G Toolbox, with the primary objective of estimating the average achievable channel capacity across varying link lengths. Key parameters under consideration include carrier frequency, antenna heights for both the Base Station (BS) and User Equipment (UE), as well as the distances between them.

Simulation Parameters: The carrier frequency (F_c) is set at 30 GHz, with the BS antenna height configured for a macro-cell scenario at 25 meters and the UE antenna height for outdoor UEs set at 1.5 meters. The simulation spans horizontal BS-UE distances (Dis2D) ranging from 50 to 300 meters, and the actual 3D BS-UE distance (Dis3D) is computed based on the specified heights and horizontal distances. Optional features such as shadow fading (Shadow Fading Flag = 1) and oxygen absorption (Oxygen Absorption Flag = 1) are incorporated, allowing for a more nuanced exploration of channel characteristics.

The simulation adopts the NR CDL-A channel model with specific configurations, including the delay profile (ITU-R M1357 Urban Macro 3D), delay spread (100 ns), carrier frequency (30 GHz), and antenna array configurations for both the BS and UE. Antenna configurations and positions for the BS and UE are obtained using the

Phased Array System Toolbox. Clustered angles (AOD, AOA, ZOD, ZOA) and subpath angles are computed based on the CDL-A model.

Capacity Estimation:

NLOS Path Loss Model: A path loss model is applied, considering the actual 3D BS-UE distance and carrier frequency. If shadow fading is enabled, a random term is added to the path loss.

Channel Coefficients Extraction: Channel coefficients are extracted using the CDL-A model and averaged over 1000 random channel realizations.

Path Loss Application: The path loss is applied to the channel coefficients.

Oxygen Absorption (Optional): If enabled, channel coefficients are further adjusted based on the oxygen absorption coefficient.

Capacity Calculation: Depending on the carrier frequency, either MIMO multiplexing or a hybrid precoding approach is employed to calculate the capacity.

Average Capacity: The average capacity is computed across all 1000 channel realizations for each link distance.

Results and Discussions

The culmination of this research is presented through a visual representation, where the average channel capacity is plotted against the horizontal distance between the BS and UE. This graphical representation illuminates the nuanced relationship between link lengths and achievable capacity in the studied wireless network scenario.

The average capacity decreases as the BS-UE horizontal distance increases. This is because the radio signal strength attenuates with distance, making it more difficult to achieve high data rates at longer distances. Additionally, the interference from other BSs and UEs can also increase with distance, further reducing the available capacity.

The graph shows that the average capacity drops below 500 Mbps at a distance of about 250 meters. This suggests that the BSs in this network deployment are spaced about 250 meters apart in order to provide good coverage and capacity to users. It is important to note that the average capacity shown in this graph is just a general trend. The actual capacity experienced by a user will depend on a number of factors, including the specific path of the radio signal between the BS and the UE, the interference environment, and the type of user equipment being used.

The figure shows the average capacity estimation with path loss effects for four different carrier frequencies (6 GHz, 30 GHz, 60 GHz, and 90 GHz) and bandwidths

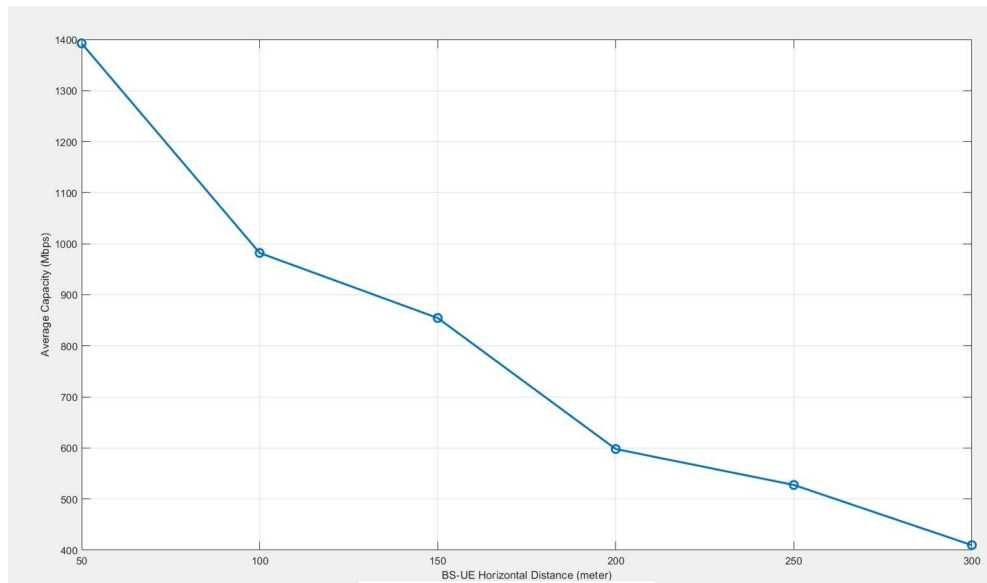


Fig. 2: Average Capacity vs. Base Station-User Equipment Horizontal Distance. The graph shows the average capacity (in Mbps) as a function of the base station (BS)-user equipment (UE) horizontal distance (in meters). The data was collected from a cellular network deployment in a suburban area.

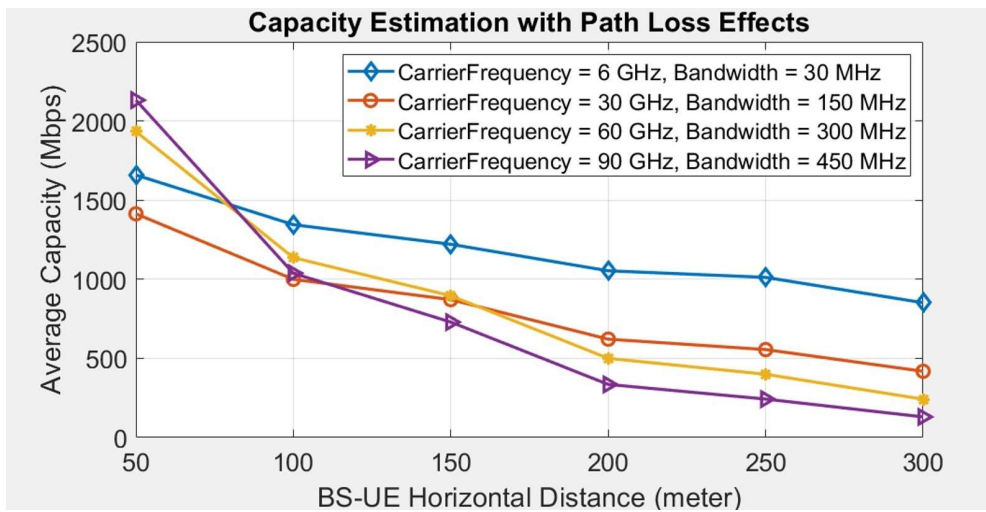


Fig. 3: Average Capacity Estimation with Path Loss Effects (30 MHz, 150 MHz, 300 MHz, and 450 MHz). The average capacity is the amount of data that can be transmitted over a given distance. The path loss effect is the reduction in signal strength as it travels through space.

As can be seen from the figure, the average capacity decreases with increasing distance between the base station (BS) and the user equipment (UE). This is due to the path

loss effect. The higher the carrier frequency, the more severe the path loss effect is. This is because higher frequency signals have shorter wavelengths and are more easily absorbed by obstacles. The bandwidth also has an impact on the average capacity. Wider bandwidths allow for more data to be transmitted simultaneously, but they also result in higher path loss.

4.1 Discussions:

The study undertaken uses the MathWorks 5G NR CDL-A channel model as a foundation for estimating channel capacity within 5G millimeter-wave bands. It is specifically designed for an urban macro-cell outdoor setting, considering a multipath delay spread of 200 nanoseconds and employing Uniform Rectangular Arrays (URAs) for both Base Station (BS) and User Equipment (UE). The adopted narrowband hybrid precoding algorithm [3] is tailored for millimeter-wave frequencies, promising realistic insights into channel behavior.

Assumptions:

Several assumptions form the basis of this research, ensuring a focused and controlled study. The chosen urban macro-cell outdoor scenario, fixed antenna gains, and the narrowband hybrid precoding algorithm are all justified decisions for the intended exploration. These assumptions collectively create a structured framework for the study's methodology, emphasizing clarity and specificity.

Simulation Requirements:

The study relies on an array of MATLAB toolboxes—Communications, DSP System, Signal Processing, 5G, and, for the channel model implementation, Phased Array System Toolbox. These software components form the backbone of the simulation infrastructure, underscoring the importance of a well-integrated and versatile computational environment.

Launcher Script and Simulation Results:

The launcher script, denoted as Average Capacity CDL A.m, serves as the director of the simulation, orchestrating the exploration of channel capacity at a predefined carrier frequency, like 30 GHz. The utilization of 1000 random channel realizations ensures robustness in the results, providing a statistical average. The simulation results are displayed for different carrier frequencies (6 GHz, 30 GHz, 60 GHz, and 90 GHz), capturing the nuances of single-link transmissions. Two instances of achievable capacity are showcased—one incorporating only path loss effects and another incorporating both path loss and oxygen absorption effects. The simulation's approximate runtime of 81 seconds attests to its efficiency in handling the defined parameters.

Comments on Capacity Estimation:

The capacity estimation methodology, rooted in the narrowband hybrid precoding approach, lays the groundwork for understanding channel behavior. It's acknowledged that this approach provides a preliminary estimate and might not capture the intricacies of wideband channels. The recommendation to adopt a precoding method with frequency selectivity for wideband channels underscores the study's commitment to precision and completeness.

Conclusions:

In conclusion, this research presents a thorough exploration of channel capacity estimation within 5G millimeter-wave bands. The chosen methodology, supported by precise assumptions, extensive simulation requirements, and a meticulously designed launcher script, provides a reliable platform for drawing meaningful conclusions. The study's engagement with the MathWorks 5G NR CDL-A channel model and its chosen hybrid precoding algorithm positions it as a valuable contribution to the understanding of channel behavior in emerging communication technologies.

Appendix A Conflicts of interest:

Authors declare that there is no Conflict of interest or competing interests.

Appendix B Code availability:

Code will be made available on reasonable request to the Authors.

Appendix C Supplementary information:

Not applicable.

Appendix D Ethical approval:

All the ethics approval was taken by an institutional review board or equivalent ethics committee.

Appendix E Funding statement:

This research has no funding associated with it.

Appendix F Competing interests:

Authors declare that there is no competing interests.

Appendix G Availability of data and materials:

Data and material will be made available on reasonable request to corresponding author.

Appendix H Ethics statements:

The authors explicitly affirm that the manuscript adheres to the following assertions: The content presented is the original work of the authors and has not been published elsewhere previously.

The manuscript is not concurrently under consideration for publication elsewhere.

The paper truthfully and comprehensively represents the author's own research and analysis.

Proper acknowledgment is given to the significant contributions of co-authors and co-researchers.

The results are appropriately situated within the context of prior and existing research.

Appendix I Author contributions:

Vaibhav Yavalkar (VY), Dr. Kamal kumar Agarwal (KA) and Dr. Sameer Nanivadekar (SN) conceptualized the project. VY conducted all simulation work, prepared the manuscript draft, and handled graphics designing. SN and KA reviewed manuscript and made corrections to the manuscript.

References

Abbas T, Qamar F, Ahmed I, et al (2017) Propagation channel characterization for 28 and 73 GHz millimeter-wave 5G frequency band. In: 2017 IEEE 15th student conference on research and development (SCOREd), pp 297–302

Al-Samman AM, Azmi MH, Al-Gumaei YA, et al (2020) Millimeter wave propagation measurements and characteristics for 5G system. *Applied Sciences* 10(1):335

Belgiovine M, Sankhe K, Bocanegra C, et al (2021) Deep learning at the edge for channel estimation in beyond-5G massive MIMO. *IEEE Wireless Communications* 28(2):19–25

Giordani M, Mezzavilla M, Rangan S, et al (2018) An efficient uplink multi-connectivity scheme for 5G millimeter-wave control plane applications. *IEEE Transactions on Wireless Communications* 17(10):6806–6821

Han S, Bian S (2020) Energy-efficient 5G for a greener future. *Nature Electronics* 3(4):182–184

Maruta K, Iwakuni T, Ohta A, et al (2016) First eigenmode transmission by high efficient CSI estimation for multiuser massive MIMO using millimeter wave bands. *Sensors* 16(7):1051

Nie S, Akyildiz IF (2019) Deep kernel learning-based channel estimation in ultra-massive MIMO communications at 0.06-10 THz. In: 2019 IEEE Globecom Workshops (GC Wkshps), pp 1–6

Thomas TA, Vook FW (2014) System level modeling and performance of an outdoor mmWave local area access system. In: 2014 IEEE 25th Annual International Symposium on Personal, Indoor, and Mobile Radio Communication (PIMRC), pp 108–112

Uwaechia AN, Mahyuddin NM (2020) A comprehensive survey on millimeter wave communications for fifth-generation wireless networks: Feasibility and challenges. *IEEE Access* 8:62367–62414

Wang HY, Cheng CH, Tsai CT, et al (2019) Multi-color laser diode heterodyned 28- GHz millimeter-wave carrier encoded with DMT for 5G wireless mobile networks. *IEEE Access* 7:122697–122706

Wen L, Yu Z, Zhu L, et al (2021) High-gain dual-band resonant cavity antenna for 5G millimeter-wave communications. *IEEE Antennas and Wireless Propagation Letters* 20(10):1878–1882

Zheng S, Han C, Huo J, et al (2021) The impact of rainfall on E-band millimeter-wave links in East China. In: 2021 XXXIVth General Assembly and Scientific Symposium of the International Union of Radio Science (URSI GASS), pp 1–4